Acta Crystallographica Section D
Biological Crystallography
ISSN 0907-4449

Zinc/calcium- and cadmium/cadmium-substituted concanavalin A: interplay of metal binding, pH and molecular packing

Julie Bouckaert,* Remy Loris and Lode Wyns

Laboratorium voor Ultrastructuur, Vlaams Interuniversitair Instituut voor Biotechnologie, Vrije Universiteit Brussel, Paardenstraat 65, B-1640 Sint-Genesius-Rode, Belgium

Correspondence e-mail: bouckaej@vub.ac.be

Received 17 July 2000
Accepted 27 September 2000

PDB References: $ZnCa^{pH6.15}$, 3enr; $CdCd^{pH5.0}$, 2enr.

The crystal structures of cadmium/cadmium and zinc/calcium concanavalin A (con A) at pH 5.0 and pH 6.15, respectively, were determined. The structure of cadmium/cadmium con A confirms that the secondary Cd^{2+}-binding site S3 is empty at pH 5. The metal-binding sites S1 and S2 are only very slightly affected by the substitution with cadmium. On the other hand, S1 and S2 and most of the protein surface of zinc/calcium con A at pH 6.15 differ from other fully metal-bound and carbohydrate-free structures. Most of these structural differences at the protein surface are a result of the interplay between metal binding, protonation and crystal packing. This interplay is expressed by relative rotations and translations of the con A units in alternative crystal packings and participation in space-group conversions inside crystals *in situ*. The particular crystal packing of zinc/calcium con A creates a novel zinc-binding site S4. The Zn^{2+} ion in S4 ligates two aspartates from one tetramer and a histidine from a symmetry-related tetramer.

1. Introduction

The *Leguminosae* lectins form a large family of closely related proteins that cover a wide range of carbohydrate specificities (Loris *et al.*, 1998). Despite the structural conservation of their monomeric units, they associate into a variety of quaternary structures, sometimes resembling those of known animal lectins (Bouckaert *et al.*, 1999; Vijayan & Chandra, 1999). At present, the crystal structures of 20 members of the legume lectin family and their complexes with various carbohydrates are available in the Protein Data Bank (Berman *et al.*, 2000), making it one of the best-studied group of carbohydrate-recognizing proteins. Of these, concanavalin A isolated from *Canavalia ensiformis* (con A) is the most extensively studied legume lectin.

The binding of metal ions in a binuclear binding site, S1 and S2, is essential for the carbohydrate-binding activity of con A (Sumner & Howell, 1936; Derewenda *et al.*, 1989) and for all legume lectins in general. Con A binds saccharides only when the active carbohydrate-binding protein is stabilized by the occupation of the calcium-binding site S2 (Bouckaert, Loris, Poortmans *et al.*, 1996). Metal-ion binding in S2 induces and maintains the *cis* isomer of the Ala207–Asp208 peptide bond characteristic of the locked form of con A and in contrast to the metal-free unlocked form of con A containing this peptide bond in the usual *trans* conformation (Bouckaert *et al.*, 1995; Brown *et al.*, 1977; Bouckaert *et al.*, 2000). Binding in S2 is itself conditional on the binding of one of several divalent metal ions [Mn^{2+}, Co^{2+}, Ni^{2+}, Cd^{2+} or Zn^{2+} (Shoham *et al.*, 1973; Bouckaert, Loris, Poortmans *et al.*, 1996); at neutral pH

Table 1
X-ray data collection and refinement statistics.

Values in parentheses are those for the highest resolution shell.

Con A species	$CdCd^{pH5.0}$ (soaked)	$ZnCa^{pH6.15}$ (co-crystal)
PDB reference	2enr	3enr
Detector	FAST	MAR IP
Data-analysis software	*MADNES*	*DENZO*
Temperature of data collection (K)	291	291
Wavelength used (Å)	1.5418	1.5418
No. of crystals	1	1
Space group	$I222$	$P2_12_12$
Unit-cell parameters (Å)		
a	63.20	60.13
b	87.69	96.46
c	89.23	87.42
Content of the asymmetric unit	Monomer	Dimer
Resolution (Å)	10.0–2.35 (2.46–2.35)	15.0–2.40 (2.49–2.40)
No. of observed reflections	30650	132328
No. of unique reflections	10111	20384
R_{merge}	0.054 (0.157)	0.103 (0.290)
Completeness (%)	95.3 (75.1)	99.4 (99.1)
$\langle I/\sigma(I)\rangle$	31.2 (10.7)	16.4 (7.3)
Reflections with $I > 3\sigma(I)$ (%)	89.7 (77.0)	93.6 (79.7)
σ cutoff used in refinement	None	None
Crystallographic R factor	0.173 (0.252)	0.215 (0.386)
R_{free}	Not evaluated	0.283 (0.455)
Bulk-solvent correction	No	Yes
R.m.s.d. bond lengths (Å)	0.019	0.014
R.m.s.d. bond angles (°)	3.1	1.8
R.m.s.d. dihedral angles (°)	28.1	27.7
R.m.s.d. impropers (°)	1.5	1.5
Ramachandran plot (non-Gly, non-Pro) (%)		
Most favourable	90.4	80.0
Additionally allowed	9.6	19.0
Generously allowed	0.0	1.0
Disallowed	0.0	0.0
No. of water molecules	99	72

also Ca^{2+} (Koenig *et al.*, 1978)] at the transition metal binding site S1. The predominant species of the naturally occurring lectin is MnCa con A; that is, fully metal-bound and locked con A where Mn^{2+} occupies the S1 site and Ca^{2+} is bound in S2.

The crystal structures of CdCd con A at pH 5 and in space group $I222$, and ZnCa con A at pH 6.15 and in space group $P2_12_12$ are presented here. They will be referred to as $CdCd^{pH5.0}$ con A and $ZnCa^{pH6.15}$ con A, respectively. These two lower pH structures will be compared with other locked fully metal-bound carbohydrate-free structures at neutral pH. A reference structure for comparison is $ZnCa^{pH7.1}$ con A. It corresponds to the same molecular species as $ZnCa^{pH6.15}$ conA, having Zn^{2+} bound at S1 and Ca^{2+} at S2, but is at a different pH and in a different crystal form (Bouckaert, Loris, Poortmans *et al.*, 1996). Other structures for comparison of, in particular, the metal-binding sites are $CdCa^{pH6.5}$ con A (PDB entry 1con; Naismith *et al.*, 1993) and $MnCa^{pH6.5}$ con A (PBD entry 2ctv; Emmerich *et al.*, 1994). The structure of unlocked $metal\text{-}free^{pH5.0}$ con A (PDB entry 1apn; Bouckaert *et al.*, 1995) is very useful to distinguish changes on the protein surface caused by the low pH or by the demetallization. This collection of con A structures enables the assignment of particular structural features to metal-ion substitutions, pH changes and/or molecular packings involved in the quaternary structure and the crystal formation of con A.

2. Material and methods

2.1. Crystallization and data collection

Metal-free con A and crystals thereof were prepared as described previously (Bouckaert *et al.*, 1995). All tools for manipulating the metal-free protein or metal-substituted protein crystals were rinsed extensively with deionized water kept in batch with Chelex-100 beads (BIORAD) prior to use, in order to prevent contamination of the protein with trace metals. All crystallization solutions were batch-treated with Chelex-100. All crystals were mounted in calcium-free borosilicate capillaries. After data collection, the metal content of the crystals was checked on a scanning electron microscope with an energy-dispersive X-ray analyzer to ensure the presence of the required metal ions and the absence of undesired ones.

$ZnCa^{pH6.15}$ con A was prepared by co-crystallization of metal-free con A with zinc and calcium. Sitting drops were composed initially of equal volumes (30 µl) of reservoir solution [1.8 *M* $(NH_4)_2SO_4$, 100 m*M* CH_3COONa pH 6.15] and protein solution (6 mg ml^{-1} of metal-free con A, 10 m*M* $ZnCl_2$ and 10 m*M* $CaCl_2$). X-ray data were collected using Rigaku RU-200 rotating-anode Cu $K\alpha$ radiation in combination with a MAR Research image-plate detector. The data were indexed and integrated with *MOSFLM*. Subsequent scaling and merging and conversion to structure factors was performed using the programs *ROTAVATA* and *AGROVATA* (Collaborative Computational Project, Number 4, 1994).

$CdCd^{pH5.0}$ con A was prepared by soaking crystals of metal-free con A for 3 h in 60 µl of the mother liquor at pH 5.0 containing 5 m*M* $CdCl_2$. The crystals thus treated were subsequently stored at 277 K for at least two weeks in borosilicate capillaries. X-ray data were collected using an Enraf–Nonius rotating-anode source operated at 40 kV, 70 mA and a FAST area detector. The data were integrated using *MADNES* (Messerschmidt & Pflugrath, 1987) and subsequently scaled and merged using *ROTAVATA* and *AGROVATA*.

2.2. Molecular replacement and refinement

The $ZnCa^{pH6.15}$ con A structure was solved by molecular replacement. A canonical dimer of the con A–mannose complex (Naismith *et al.*, 1994) was used as the search model, resulting in an initial correlation factor of 0.40 and a crystallographic R factor of 0.52. Refinement was carried out entirely with *X-PLOR* (Brünger, 1992). After an initial slow-cool stage (3000 K) to remove potential model bias, the R factor dropped to 0.26 and the free R factor (Brünger, 1997) to 0.33. At this stage, electron densities were inspected and the metal ions were added to the structure. This was followed by alternating rounds of manual rebuilding and restrained positional and B-factor refinement (without any σ cutoffs and

updating the bulk-solvent correction after each refinement round or rebuilding session). The refinement of the ZnCa$^{pH6.15}$ con A structure was evaluated by cross-correlation using R_{free}; a bulk-solvent correction was applied and updated throughout the refinement.

Refinement of CdCd$^{pH5.0}$ con A started from the coordinates for the isomorphous structure of CdCa con A at 1.85 Å (PDB entry 1con). After an initial rigid-body refinement, positional and individual *B*-factor refinements were performed as for the ZnCa$^{pH6.15}$ con A structure except that no free *R* factor was used. This is because CdCd$^{pH5.0}$ con A was originally refined when R_{free} or bulk-solvent correction were not yet in common use.

For both structures, no metal–ligand bond-distance restraints were employed and the metal ions were given no charge. Water molecules were added only if (i) the water had at least one hydrogen-bonding partner, (ii) the positive difference density level was higher than 3σ and (iii) after refinement the electron density of the putative water reappeared in the $2F_o - F_c$ map at a level of at least 1σ.

3. Results and discussion

Both CdCd$^{pH5.0}$ con A and ZnCa$^{pH6.15}$ con A are locked carbohydrate-binding structures of con A containing the unusual *cis* peptide bond between Ala207 and Asp208. The data collection, refinement statistics and the final number of water molecules are shown in Table 1. The overall structure of con A consisting of a β-sandwich (Fig. 1) is conserved and will not be discussed in further detail.

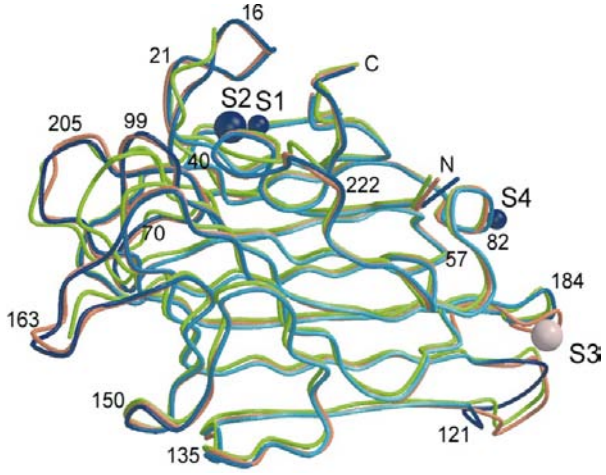

Figure 1
Three-dimensional structure of the con A monomer. Overlay of the crystal structures of ZnCa$^{pH6.15}$ con A (blue, colour ramped from light to dark blue for low to high temperature factors; PDB entry 3enr), CdCd$^{pH5.0}$ con A in orange (PDB entry 2enr) and metal-free$^{pH5.0}$ con A in green (PDB entry 1apn) *via* superposition of the 119 β-sheet residues of con A. The metal ions of ZnCa$^{pH6.15}$ con A, where zinc and calcium occupy the S1 and S2 sites, respectively, are displayed as blue spheres. A secondary Zn^{2+}-binding site S4 is created by the crystal packing. The packing-independent Cd^{2+}-binding site S3 is empty in the structure of CdCd$^{pH5.0}$ con A at pH 5. Residues at discussed loops are numbered to allow the localization of these loops.

3.1. Overall structure of CdCd$^{pH5.0}$ con A

CdCd$^{pH5.0}$ con A has cadmium bound in both metal-binding sites S1 and S2 (Fig. 2*a*). It originates from crystals of metal-free unlocked con A, which after soaking with cadmium for two weeks at 277 K convert from space group $P2_12_12$ to $I222$. With this space-group conversion, the asymmetric unit changes from a dimer to a monomer and the protein obtains its active 'locked' conformation. The locking of the structure coincides with a space-group conversion with an increase in crystallographic symmetry (Figs. 3*b* and 3*c*).

The structure of CdCd$^{pH5.0}$ con A is most similar to CdCa$^{pH6.5}$ con A (Fig. 4), with an r.m.s. difference for the main-chain atoms of the 119 β-sheet residues of 0.10 Å. The r.m.s. deviation increases for isomorphous structures at still higher pH values (*e.g.* 0.19 Å with ZnCa$^{pH7.1}$ con A). The overall temperature factors of CdCd$^{pH5.0}$ con A are higher than for con A structures at neutral pH. The most plausible factor causing these differences between isomorphous low and neutral pH structures of con A is dissociation of the con A tetramers into dimers below pH 6.5 (Bouckaert, Loris & Wyns,

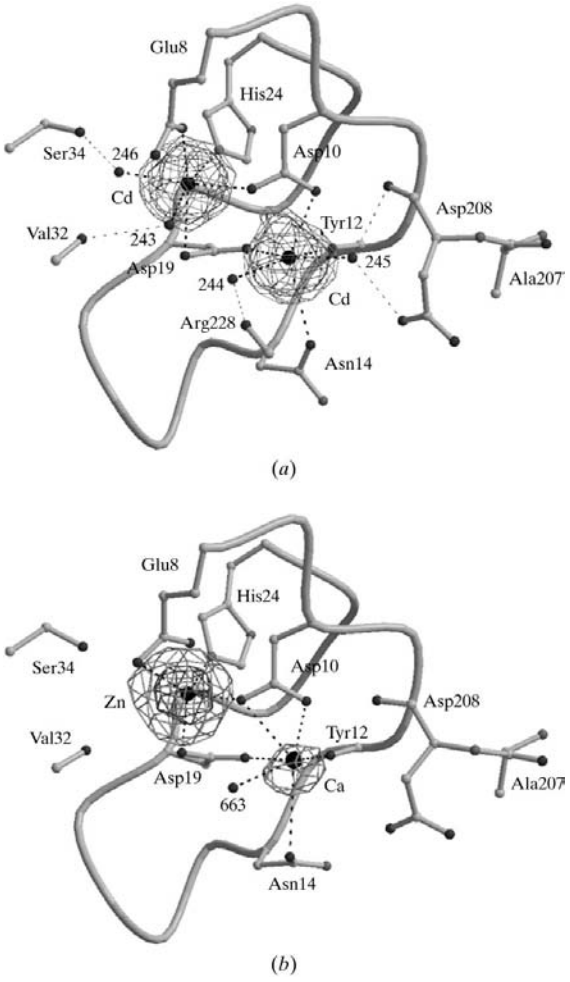

Figure 2
Metal-binding sites S1 and S2. (*a*) CdCd$^{pH5.0}$ con A. (*b*) ZnCa$^{pH6.15}$ con A. Shown are the omit electron densities contoured at 5 and 10 $\sigma(F_o - F_c)$ and ball-and-stick models of the metals and ligand residues.

Table 2
Metal–ligand distances (Å) at S1 and S2.

Temperature factors (Å^2) of the ligands are given in parentheses. ZnCa1 and 2 represent the two monomers in the asymmetric unit.

	ZnCa$^{pH7.1}$	ZnCa1$^{pH6.15}$	ZnCa2$^{pH6.15}$	MnCa$^{pH6.5}$	CdCd$^{pH5.0}$	CdCa$^{pH6.5}$
Transition metal binding site S1						
Metal ion	Zn (11)	Zn (60)	Zn (44)	Mn (15)	Cd (29)	Cd (14)
Glu8 OE2	2.19 (8)	2.46 (48)	2.40 (46)	2.23 (14)	2.54 (17)	2.33 (16)
Asp10 OD2	2.11 (7)	2.36 (29)	2.05 (19)	2.13 (15)	2.32 (27)	2.14 16)
Asp19 OD1	2.22 (12)	2.58 (62)	2.54 (49)	2.26 (13)	2.82 (33)	2.40 (17)
His24 NE2	2.11 (7)	2.40 (32)	2.20 (29)	2.25 (9)	2.33 (21)	2.34 (13)
Wat O	2.30 (10)	—	—	2.26 (14)	2.26 (23)	2.50 (16)
Wat O	2.21 (9)	—	—	2.13 (9)	2.57 (30)	2.13 (13)
Average	2.19 (9)	2.45 (43)	2.30 (36)	2.21 (12)	2.47 (25)	2.31 (14)
Calcium binding site S2						
Metal ion	Ca (8)	Ca (76)	Ca (52)	Ca (10)	Cd (32)	Ca (11)
Asp19 OD2	2.38 (9)	2.39 (43)	2.79 (49)	2.30 (11)	2.42 (28)	2.30 (12)
Asp10 OD2	2.46 (7)	2.65 (29)	3.20 (19)	2.45 (15)	2.69 (27)	2.29 (13)
Asp10 OD1	2.38 (9)	2.60 (40)	2.47 (42)	2.28 (10)	2.42 (23)	2.52 (16)
Asn14 OD1	2.52 (12)	2.99 (78)	2.81 (72)	2.55 (15)	3.09 (32)	2.60 (17)
Tyr12 O	2.30 (9)	2.87 (53)	2.28 (55)	2.31 (10)	2.42 (32)	2.32 (13)
Wat O	2.35 (8)	—	—	2.37 (10)	2.70 (34)	2.35 (13)
Wat O	2.42 (8)	—	—	2.32 (12)	2.83 (29)	2.50 (16)
Average	2.40 (9)	2.70 (49)	2.71 (47)	2.37 (12)	2.65 (29)	2.41 (13)
S1–S2 distance	4.16	4.59	4.69	4.16	4.21	4.18

1996). In solution at pH values between 5 and 7, a mixture of dimers and tetramers is observed (Senear & Teller, 1981*a*).

The CdCd$^{pH5.0}$ con A structure does not contain a Cd^{2+} ion bound to the S3 site (Figs. 1 and 3) as identified earlier in the structure of CdCa$^{pH6.5}$ con A (Naismith *et al.*, 1993), and the S3 ligand Asp136, Glu87 and Glu183 have their native side-chain conformation. Cd^{2+} binding at S3 was correlated with stabilization of con A by recent microcalorimetric measurements (Sanders *et al.*, 1998). The stabilization is removed below pH 6.4, where no Cd^{2+} is bound at S3 (Sanders *et al.*, 1998), in agreement with the CdCd$^{pH5.0}$ con A structure. Above this pH, a structure of CdCd con A with a filled S3 site could exist, confirming previous NMR results of the binding of three cadmium ions per con A molecule (Palmer *et al.*, 1980). The S3 site is located closely to the con A dimer interface (Fig. 3), but is not involved in crystal packing.

3.2. Overall structure of ZnCa$^{pH6.15}$ con A

The ZnCa$^{pH6.15}$ con A crystals were grown by co-crystallization of metal-free unlocked con A with zinc and calcium ions. ZnCa$^{pH6.15}$ con A shows significant deviations in some surface loops both from the structures of ZnCa$^{pH7.1}$ con A (PDB entry 1enr) and of metal-free$^{pH5.0}$ con A (PDB entry 1apn) (Figs. 1 and 4). The r.m.s. deviations for the main-chain atoms of the 119 β-sheet residues of ZnCa$^{pH6.15}$ con A compared with ZnCa$^{pH7.1}$ con A (0.35 Å) and metal-free$^{pH5.0}$ con A (0.28 Å) are higher than is usual among con A crystal structures. For comparison, typical r.m.s. differences for the same atoms among isomorphous crystals of different metal-ion substituted con As vary

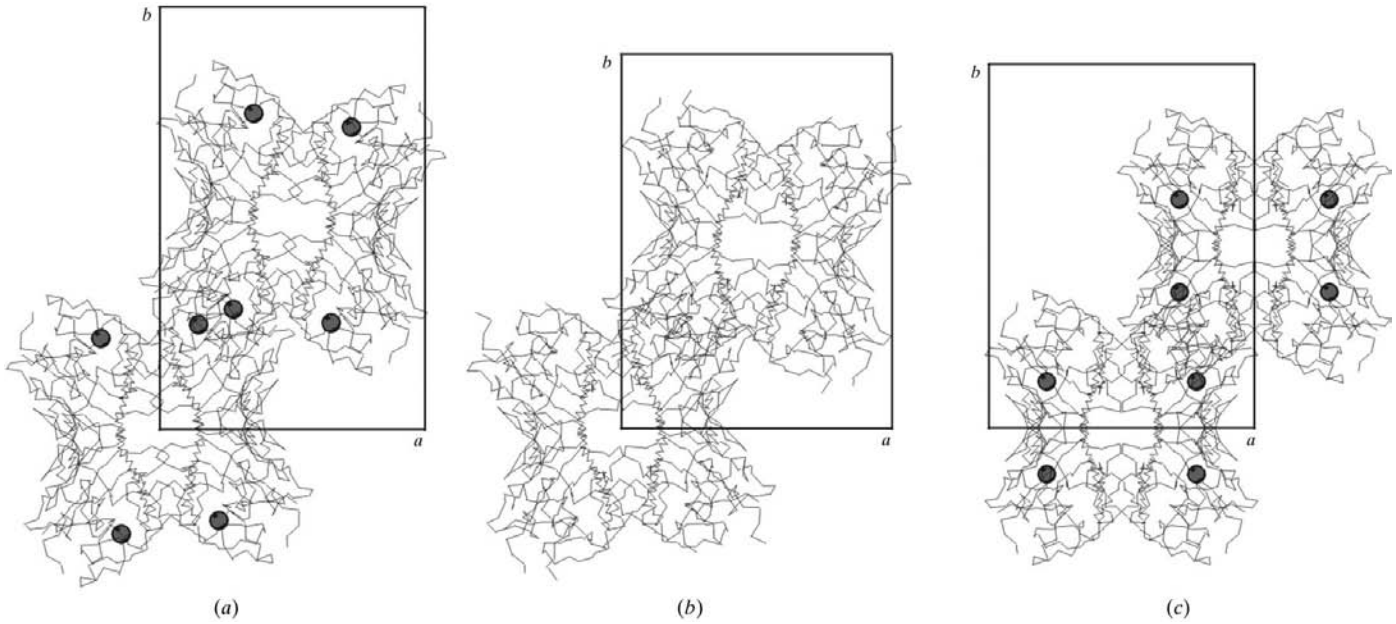

Figure 3
Crystal packing of *(a)* ZnCa$^{pH6.15}$ con A, $P2_12_12$, (*b*) metal-free$^{pH5.0}$ con A $P2_12_12$, (*c*) CdCd$^{pH5.0}$ con A, $I222$. The location of the secondary Zn^{2+} site S4 in *(a)* and the secondary Cd^{2+} site S3 in (*c*) are indicated by small black spheres. The 222 point-group symmetry of the con A tetramers in the $I222$ crystals coincides with the crystallographic symmetry. In contrast, in metal-free$^{pH5.0}$ con A and ZnCa$^{pH6.15}$ con A crystals the tetramers are rotated 7° around the crystallographic z axis. ZnCa$^{pH6.15}$ con A also undergoes a rather large translation along the b unit-cell dimension.

between 0.10 and 0.19 Å. Between non-isomorphous con A structures, larger r.m.s. differences ranging from 0.19 to 0.24 Å are typically observed. The temperature factors of the $ZnCa^{pH6.15}$ con A dimer are also high overall compared with $ZnCa^{pH7.1}$ con A or even the unlocked metal-free$^{pH5.0}$ con A (Table 2).

Structural differences that do not involve con A tetramer formation (see below) are located at Ser21 and in the loops Ser160–Pro165, Ser223–Ser225, Lys135–Asp136, Thr148–Asp151, Pro202–Pro206 and Leu81–Asn83 (Figs. 1 and 4). Since the pH of crystallization of $ZnCa^{pH6.15}$ con A is intermediate between that of metal-free$^{pH5.0}$ con A and $ZnCa^{pH7.1}$ con A, these differences are most likely to reflect the combined effects of the crystal environment and pH on these solvent-exposed loops.

The side-chain hydroxyl group of Ser21 is in a packing contact with Lys135 N^{ζ} in $ZnCa^{pH7.1}$ con A crystals. This interaction is absent in both metal-free$^{pH5.0}$ con A and $ZnCa^{pH6.15}$ con A. Exclusively in $ZnCa^{pH6.15}$ con A crystals, Ser223 O^{γ} interacts with Asp136 $O^{\delta2}$. Both changes are because of a different relative orientation of the con A molecules in the crystal packing. The surface loops Ser160–Pro165 and Thr148–Asp151 are not involved in any packing contact, but are ill-determined by the electron density. The two other loops, Pro202–Pro206 and Leu81–Asn83, are involved in the formation of a secondary binding site for Zn^{2+}. This novel Zn^{2+}-binding site is created at the interface of two tetramers of $ZnCa^{pH6.15}$ con A and will be discussed in detail below.

The crystal packing of $ZnCa^{pH6.15}$ con A is related to those of metal-free con A and $ZnCa^{pH7.1}$ con A. Compared with $ZnCa^{pH7.1}$ con A, the con A tetramers in the $ZnCa^{pH6.15}$ con A crystals undergo a small rotation of 7° around z as well as a translation that creates an alternative crystal packing (Fig. 3). A similar rotation is observed in the structure of metal-free$^{pH5.0}$ con A; however, the translational component is different. This rotation changes the space-group symmetry from $I222$ to $P2_12_12$ and leaves the z axis as the only crystallographic twofold axis.

3.3. Structural consequences of the metal-ion substitutions

In $CdCd^{pH5.0}$ con A, the identity of the Cd^{2+} ions in both S1 and S2 was obvious from the strong electron density (Fig. 2*a*), involving 46 electrons compared with 18 electrons for Ca^{2+} and 23 electrons for Mn^{2+}. The structural impact of the metal-ion substitution relative to native con A ($MnCa^{pH6.5}$ con A) or other isomorphous structures (*e.g.* $CdCa^{pH6.5}$ con A, $ZnCa^{pH7.1}$ con A) remains limited to the metal-binding sites S1 and S2. $CdCd^{pH5.0}$ con A metal–ligand distances are increased significantly (Table 2) compared with $MnCa^{pH6.5}$ con A or $ZnCa^{pH7.1}$ con A. In S1 as well as in S2 the Cd^{2+} ion extends its coordination shell. This may be a consequence of the lack of ligand-field stabilization energy because of the filled *d* shell of Cd^{2+}. In contrast, the internuclear S1–S2 distance between the Cd^{2+} ions is however only slightly increased (Table 2). This supports the structural preservation of the binuclear metal-binding site in con A, despite the substitutions with Cd^{2+}, and is in agreement with the finding that the coordination of structures with Cd^{2+} substituted for Ca^{2+} are mostly found to be identical to the coordination in the Ca^{2+}-bound protein (Glusker, 1991). In conclusion, Cd^{2+} can replace Ca^{2+} efficiently.

In $ZnCa^{pH6.15}$ con A, the coordination shells of the Zn^{2+} and Ca^{2+} ions in S1 and S2 are essentially identical to those in $ZnCa^{pH7.1}$ con A (Fig. 2*b*; Emmerich *et al.*, 1994). However, the electron densities of the side chains ligating the two metal ions are not always well defined. On average, smaller metal–ligand distances are expected in S1 for Zn^{2+} than for Mn^{2+} (Glusker, 1991). This is indeed the case in the structure of $ZnCa^{pH7.1}$ con A

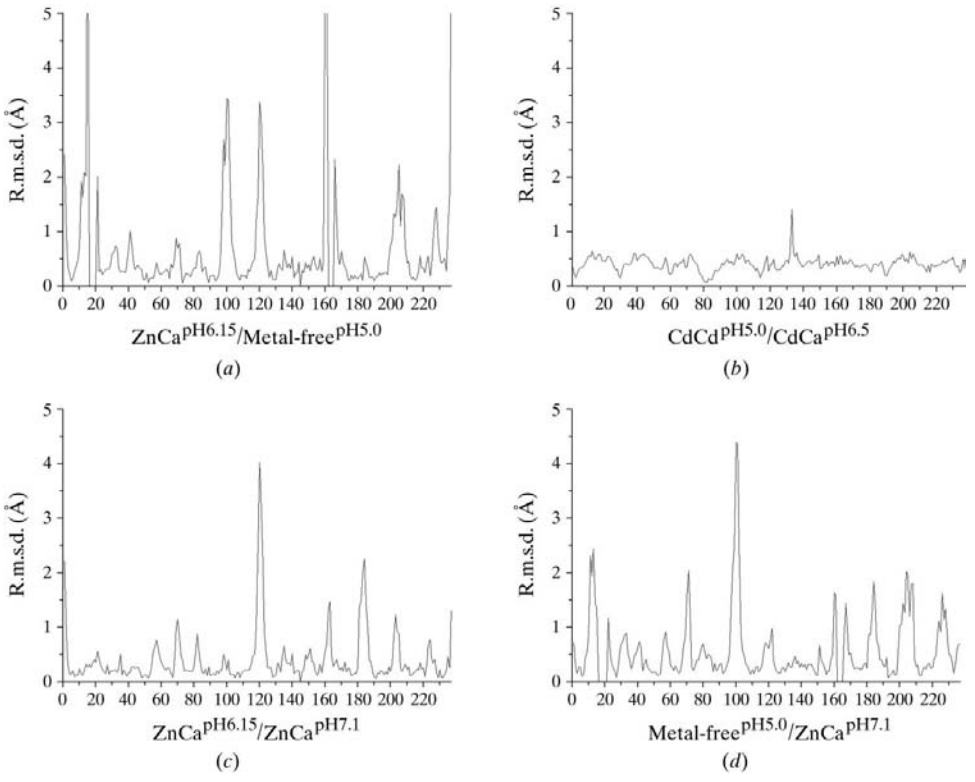

Figure 4
Plots of the r.m.s. deviations per residue number between (*a*) $ZnCa^{pH6.15}$ con A and metal-free$^{pH5.0}$ con A, (*b*) $CdCd^{pH5.0}$ con A and $CdCa^{pH6.5}$ con A, (*c*) $ZnCa^{pH6.15}$ con A and $ZnCa^{pH7.1}$ con A and (*d*) metal-free$^{pH5.0}$ con A and $ZnCa^{pH7.1}$ con A. Residues 16–21 and 162–165 are not included in the metal-free con A structure.

compared with that of MnCa$^{pH6.5}$ con A. The contrary is true in ZnCa$^{pH6.15}$ con A (Table 2). The metal–ligand distances for the Ca^{2+} ion in S2 have also increased (Table 2) and are even larger than for Cd^{2+} in S2 in CdCd$^{pH6.5}$ con A. The S1–S2 distance is significantly larger than in MnCa$^{pH6.5}$ con A or ZnCa$^{pH7.1}$ con A. Thus, the metal-binding sites in crystals of ZnCa$^{pH6.15}$ con A appear much more disturbed than in other carbohydrate-free crystal structures of con A containing different metal ions in S1 (Emmerich *et al.*, 1994). The latter crystals all have space group *I*222, in which crystal packing interactions further stabilize the metal- and carbohydrate-binding region (Bouckaert *et al.*, 2000).

3.4. A novel Zn^{2+}-binding site in ZnCa$^{pH6.15}$ con A

The crystal packing of the ZnCa$^{pH6.15}$ con A crystals involves a secondary Zn^{2+}-binding site (Fig. 5*a*) at the interface of two tetramers of ZnCa$^{pH6.15}$ con A. This novel Zn^{2+}-binding site will be referred to as site S4. S4 is distinct from the two major metal-binding sites S1 and S2 and is also distinct from the Cd^{2+}-binding site S3 identified by Naismith and colleagues inside the subunit structure of CdCa con A (Naismith *et al.*, 1993; Fig. 1). The Zn^{2+}-binding site is generated by the translation of two ZnCa$^{pH6.15}$ con A tetramers 5 Å away from each other when compared with the molecular packing in metal-free$^{pH5.0}$ con A crystals (Fig. 3). The translation is in the direction of the crystallographic *b* axis and leads to a larger *b* unit-cell parameter in ZnCa$^{pH6.15}$ con A crystals.

Two surface loops, Pro202–Pro206 and Leu81–Asn83, are involved in the formation of S4, as mentioned above. The Zn^{2+} ion is ligated by the carboxylate groups of Asp80 and Asp82 and by the N$^{\varepsilon 2}$ atom of the symmetry-related histidine His205 of the neighbouring tetramer (Fig. 5*a*) in both monomers present in the asymmetric unit of ZnCa$^{pH6.15}$ con A.

In both metal-free$^{pH5.0}$ con A and ZnCa$^{pH7.1}$ con A (Fig. 5*c*), the side chain of His205 is too far removed to create the same S4 binding site as in ZnCa$^{pH6.15}$ con A. However, when metal-free$^{pH5.0}$ con A crystals are soaked with Mn^{2+} (PDB entry 1dq4), an Mn^{2+} ion is bound at Asp80 and Asp82 (Fig. 5*b*). In this structure, the complementing His205 is replaced by Asp203 in one of two non-crystallographically related sites (Fig. 5*b*). These Mn^{2+}-binding sites are present in their actual form in metal-free$^{pH5.0}$ con A crystals so that the ions can instantly fill the sites. In the second monomer, Asp80 and Asp82 alone constitute the Mn^{2+}-binding site and His205 makes a hydrogen bond to Asp82. This hydrogen bond is also found in the related Zn^{2+}- and Co^{2+}-soaked metal-free$^{pH5.0}$ con A crystals (PDB entries 1ces and 1ens; Bouckaert, Loris, Poortmans *et al.*, 1996). The latter structures contain almost no Zn^{2+} or Co^{2+} at the S4 site between Asp80, Asp82 and Asp203. Apparently, the Mn^{2+} site, which is composed solely of aspartate side chains, is less suitable for Zn^{2+} or Co^{2+} ions. Interestingly, this structure will further change to MnMn con A over a longer time period by rotation of the con A tetramers to gain crystallographic 222 symmetry. Asp80 and Asp82 are thereby separated from His205, similar to in ZnCa$^{pH7.1}$ con A (Fig. 5*c*) where no Zn^{2+} ion can be bound at S4.

An earlier X-ray absorption fine-structure investigation has described the Zn^{2+} ion in S1 in a polycrystalline slurry of ZnCa con A prepared at pH 6.5 (Lin *et al.*, 1990). These authors found a lower than six Zn^{2+} coordination number, different from the coordination number calculated from solution EXAFS studies, and concluded that the crystal lattice may

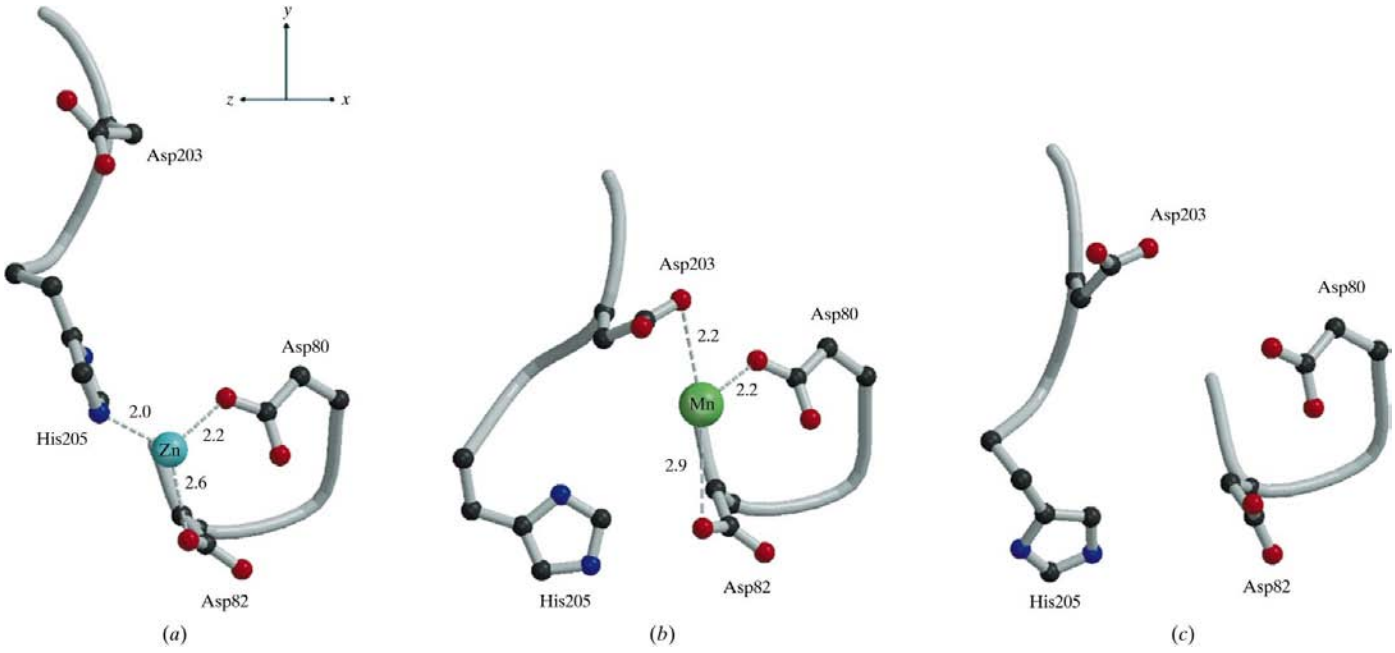

Figure 5
The crystal environment of the zinc-binding site S4. (*a*) ZnCa$^{pH6.15}$ con A, (*b*) corresponding view of metal-free$^{pH5.0}$ con A soaked with Mn^{2+} (PDB entry 1dq4), (*c*) ZnCa$^{pH7.1}$ con A (PDB entry 1enr).

Table 3
Intersubunit hydrogen bonds between two dimers that create the con A tetramer in the crystal.

Hydrogen bond	Metal-free$^{pH5.0}$		CdCd$^{pH5.0}$	ZnCa$^{pH6.15}$		ZnCa$^{pH7.1}$
Ser62 O$^{\gamma}\cdots$Asp58 O$^{\delta1}$	2.65	2.72	2.77	2.57	2.63	2.57
His121 N$^{\varepsilon2}\cdots$Ser108 O$^{\gamma}$	2.93	2.93	3.21	—	—	2.90
His121 N$^{\varepsilon2}\cdots$Asn131 O$^{\delta1}$	—	—	—	2.74	3.11	—
Lys116 N$^{\zeta}\cdots$Glu192 O$^{\varepsilon2}$	—	—	—	2.56	2.63	2.93
Asn69 N$\cdots$Asn118 O $^{\delta1}$	—	2.85	—	—	—	
Ala70 O$\cdots$Asn118 N$^{\delta2}$	—	—	—	—	—	3.47

have a profound effect on the structure of the metal-binding sites. Our results suggest another explanation of the differences found between EXAFS data derived from solution studies and from the solid state. The crystal form present in the polycrystalline slurry used by Lin and coworkers was not characterized, but is likely to correspond to the crystal form described in the present paper. If in the polycrystalline slurry crystal packing is indeed mediated by a second Zn^{2+}-binding site, similar to the S4 site found in ZnCa$^{pH6.15}$ con A, the EXAFS spectra from these crystals around the Zn^{2+} absorption edge would deviate significantly from those of ZnCa con A in solution, even if the Zn^{2+} binding in the S1 site is identical. The EXAFS-derived average Zn^{2+}–ligand distance is probably significantly more accurate than the crystallographic distance, but is inevitably a weighted average over all Zn sites. In fact, a correct interpretation of the EXAFS results by simulation from ZnCa$^{pH6.15}$ con A crystals would be impossible owing to the inability to separate the contributions of the two different Zn^{2+} binding sites S1 and S4.

3.5. Contacts at the tetramer interface

Con A is known to behave as a dimer in solution below pH 5.0 and as a tetramer above pH 7.0. At intermediate pH values, a mixture of dimers and tetramers is present (Senear & Teller, 1981*a*). The pH dependence of the dimer–tetramer equilibrium of con A is of interest because some biological properties of con A have been shown to depend on the valency of con A for saccharide ligands (Mandal & Brewer, 1993). Senear & Teller (1981*b*) studied the dimer–tetramer equilibrium thermodynamically and found that tetramer association is governed by the ionization of a histidine side chain on each of the subunits, either His51 or His121. The protonation of the four His121 residues that are located closely together in the tetramer is thought to cause a charge repulsion and dissociation of the dimers. In the crystal structures of CdCd$^{pH5.0}$ con A, ZnCa$^{pH6.15}$ con A and metal-free$^{pH5.0}$, crystal packing generates a tetramer similar to that found in the high-pH crystal structures of con A. Hydrogen bonds mediating tetramer formation in different crystal structures of con A are given in Table 3. We find that His121 makes the same interactions in CdCd$^{pH5.0}$ con A, ZnCa$^{pH7.1}$ con A and metal-free$^{pH5.0}$ con A. It behaves differently only in ZnCa$^{pH6.15}$ con A, where its hydrogen bond with Ser108 is replaced by an alternative one with Asn131.

Residues Asn69 and Ala70 on the surface of the six-stranded back β-sheet (Fig. 1), which mediate tetramer formation with loop Asn118–Thr123 of the opposing dimer in the *I*222 con A crystal form (CdCd$^{pH5.0}$ con A as well as ZnCa$^{pH7.1}$ con A; Table 3), are less well defined by the electron density in ZnCa$^{pH6.15}$ con A. This is probably a consequence of ZnCa$^{pH6.15}$ con A lacking these extra stabilizing symmetry contacts.

In addition to the hydrogen bonds listed in Table 3, a salt bridge across the tetramer interface is observed involving Asp58 and Arg60. This interaction does not have good hydrogen-bond geometry, but the distance between both charged groups is sufficiently small to assume it to be energetically favourable. This salt bridge is disrupted in all structures below pH 6.5 because of a different side-chain conformation of Arg60. This coincides with a slightly different intersubunit orientation in the con A tetramer.

We thank the Fund for Scientific Research–Flanders (FWO) for the funding of its postdoctoral research fellows RL and JB. Yves Geunes was of great help in preparing the figures. We further acknowledge the Vlaams Interuniversitair Instituut voor Biotechnologie (VIB) for financial support.

References

Berman, H. M., Westbrook, J., Feng, Z., Gilliland, G., Bhat, T. N., Weissig, H., Shindyalov, I. N. & Bourne, P. E. (2000). *Nucleic Acids Res.* **28**, 235–242.
Bouckaert, J., Dewallef, Y., Poortmans, F., Wyns, L. & Loris, R. (2000). *J. Biol. Chem.* **275**, 19778–19787.
Bouckaert, J., Hamelryck, T. W., Wyns, L. & Loris, R. (1999). *Curr. Opin. Struct. Biol.* **9**, 572–577.
Bouckaert, J., Loris, R., Poortmans, F. & Wyns, L. (1995). *Proteins Struct. Funct. Genet.* **23**, 510–524.
Bouckaert, J., Loris, R., Poortmans, F. & Wyns, L. (1996). *J. Biol. Chem.* **271**, 16144–16150.
Bouckaert, J., Loris, R. & Wyns, L. (1996). *Lectins Biol. Biochem. Clin. Biochem.* **11**, 50–60.
Brown, R. D. I., Brewer, C. F. & Koenig, S. H. (1977). *Biochemistry*, **16**, 3883–3896.
Brünger, A. T. (1992). *X-PLOR. Version 3.1. A System for X-ray Crystallography and NMR.* Yale University, Connecticut, USA.
Brünger, A. T. (1997). *Methods Enzymol.* **277**, 366–396.
Collaborative Computational Project, Number 4 (1994). *Acta Cryst.* D**50**, 760–763.
Derewenda, Z., Yariv, J., Helliwell, J. R., Kalb (Gilboa), A. J., Dodson, E. J., Papiz, M. Z., Wan, T. & Campbell, J. (1989). *EMBO J.* **8**, 2189–2193.
Emmerich, C., Helliwell, J. R., Redshaw, M., Naismith, J. H., Harrop, S. J., Raftery, J., Kalb (Gilboa), A. J., Yariv, J., Dauter, Z. & Wilson, K. S. (1994). *Acta Cryst.* D**50**, 749–756.
Glusker, J. P. (1991). *Adv. Protein Chem.* **42**, 3–76.
Koenig, S. H., Brewer, C. F. & Brown, R. D. I. (1978). *Biochemistry*, **17**, 4251–4260.
Lin, S.-L., Stern, E. A., Kalb (Gilboa), A. J. & Zhang, Y. (1990). *Biochemistry*, **29**, 3599–3603.
Loris, R., Hamelryck, T., Bouckaert, J. & Wyns, L. (1998). *Biochim. Biophys. Acta*, **1383**, 9–36.
Mandal, D. K. & Brewer, C. F. (1993). *Biochemistry*, **32**, 5116–5120.

Messerschmidt, A. & Pflugrath, J. W. (1987). *J. Appl. Cryst.* **20**, 306–315.
Naismith, J. H., Emmerich, C., Habash, J., Harrop, S. J., Helliwell, J. R., Hunter, W. N., Raftery, J., Kalb (Gilboa), J. & Yariv, J. (1994). *Acta Cryst.* D**50**, 847–858.
Naismith, J. H., Habash, J., Harrop, S. J., Helliwell, J. R., Hunter, W. N., Wan, T. C. M. & Weisgerber, S. (1993). *Acta Cryst.* D**49**, 561–571.
Palmer, A. R., Bailey, D. B., Behnke, W. D., Cardin, A. D., Yang, P. P. & Ellis, P. D. (1980). *Biochemistry*, **19**, 5063–5070.
Sanders, J. N., Chenoweth, S. A. & Schwartz, F. P. (1998). *J. Inorg. Biochem.* **70**, 71–82.
Senear, D. F. & Teller, D. C. (1981*a*). *Biochemistry*, **20**, 3076–3083.
Senear, D. F. & Teller, D. C. (1981*b*). *Biochemistry*, **20**, 3083–3091.
Shoham, M., Kalb, A. J. & Pecht, I. (1973). *Biochemistry*, **12**, 1914–1917.
Sumner, J. B. & Howell, S. F. (1936). *J. Biol. Chem.* **115**, 583–588.
Vijayan, M. & Chandra, N. R. (1999). *Curr. Opin. Struct. Biol.* **9**, 707–714.